An Investigation of the Roles of Surface Aluminum and Acid Sites in the Zeolite MCM-22

Ding Ma,[a] Xiuwen Han,[a] Sujuan Xie,[a] Xinhe Bao,*[a] Hongbing Hu,[b] and Steve C. F. Au-Yeung*[b]

Abstract: Ammonia adsorption studies reveal that the observed Lewis acidity in the zeolite MCM-22 is derived from at least two types of framework aluminum sites (Al^F), that is, octahedral Al^F and three-coordinate Al^F. Comparative ammonia or trimethylphosphine (TMP) adsorption experiments with MCM-22 confirm that octahedral Al species gives rise to the signal at $\delta_{iso} \approx 0$ in the ^{27}Al NMR spectrum; this is a superposition of two NMR signals from the different Al species on the water-reconstructed zeolite surface. A sharp resonance assigned to framework Al reversibly transforms on ammonia adsorption to δ_{iso} $^{27}Al \approx 55$ from tetrahedral Al^F, while the broad peak is assigned to nonframework aluminum which results from hydrothermal treatment. This study also demonstrates the effectiveness of ^{27}Al magic angle spinning (MAS) and multiple quantum (MQ) MAS NMR spectroscopy as a technique for the study of zeolite reactions.

Keywords: aluminum · Lewis acids · NMR spectroscopy · zeolites

Introduction

Aluminum within zeolites plays a key role in catalytic reactions. The location of Al within the zeolite structure determines its function, for example, as Brønsted or Lewis acid sites. The acid properties of zeolites depend on the site, the geometry, and the coordination number of Al in the zeolites.[1–4] Therefore, identification of acidic sites in zeolites and measurement of their acidities is important in the study of acid-catalyzed reactions.[5, 6]

MCM-22 is a new family of high-siliceous zeolite, which possesses two types of channel systems[7–12] and has been shown to be a good catalyst for various catalytic reactions, such as disproportionation,[13] methane aromatizaion,[14] and isomerization of butene[15]. Recently, we completed the characterization of the dealumination process of MCM-22,[16] and the results suggest that its dealumination differs from zeolites with low Si/Al ratios such as Y. In short, the second step in the zeolite dealumination model proposed by Kuhl does not occur, and this leaves three-coordinate Al^F and distorted tetrahedral Al^F sites in the zeolite. The former gives rise to the broad hump ($\delta \approx 100-150$) observed in the ^{27}Al MAS NMR spectrum of a sample that is fully hydrated, whereas signals from the latter remain unresolved.

Despite the complexity which results from quadrupolar interactions at Al ($I = 5/2$), the results of previous ^{27}Al MAS NMR spectroscopic measurements revealed that the Brønsted acid sites can be described as framework-bridging hydroxyl groups[5] (Si–OH–Al, tetrahedral species with NMR signals at $\delta = 50-65$), which release Brønsted protons during proton-transfer reactions.[17] Probe molecules such as pyridine and ammonia have been used to obtain information on Lewis acid sites in zeolites by IR studies. Suggestions for the nature of the Lewis acid sites vary from three-coordinate silicon,[18] Al–O species on extra-lattice positions,[19] pentagonal sites in Al^{NF} (nonframework aluminum) debris,[20] to octahedral Al^{NF} in most cases. Although combined ^{27}Al MAS and cross polarization (CP)/MAS NMR methods have been demonstrated to be highly effective in revealing the presence of Al species in a water-reconstructed sample, the nature of Al species on "surface" zeolites remains elusive as water chemisorbs dissociatively and provokes extensive surface reconstruction.[20, 21] Therefore, indentification and charaterization of the structure of the Al species that possess Lewis acidity remains inconclusive.

Among the different molecules which have been applied to study the variation in acidity[21–25] of zeolite sites, pyridine,[21] trimethylphosphine (TMP),[23] NH_3,[26] and triethlphosphine oxide[27] have proven to be efficient probes. In particular, TMP and NH_3 are widely used as probes in NMR or IR

[a] Prof. X. Bao, D. Ma, Prof. X. Han, S. Xie
State Key Laboratory of Catalysis
Dalian Institute of Chemical Physics
Chinese Academy of Sciences
Dalian 116023 (China)
Fax: (86) 4-114-694-447
E-mail: xhbao@dicp.ac.cn

[b] Prof. S. C. F. Au-Yeung, H. Hu
Department of Chemistry
The Chinese University of Hong Kong
Shatin N. T. (Hong Kong)

Supporting information for this article is available on the WWW under http://wiley-vch.de/home/chemistry/ or from the author.

0947-6539/02/0801-0162 $ 17.50+.50/0

spectroscopy for the characterization of the acidity of zeolites.[23, 25, 28–31] The pioneering study by Lunsford et al.[23] demonstrated the feasibility of distinguishing Brønsted sites from Lewis acid sites by using TMP as a probe molecule. When adsorbed on Lewis sites (L) or on Brønsted sites they form either the probe-L or probe–H^+ adducts, and can be distinguished by the differences in their corresponding ^{15}N or ^{31}P chemical shifts. Fripiat et al. reported that the ^{27}Al MAS and CP/MAS NMR spectra of Y-type zeolites, after adsorption of NH_3, provided unique information on the non-reconstructed surface of the zeolites,[20] thereby advancing the understanding of the chemical integrity of Al species in zeolite reactions. It is well recognized that ^{27}Al NMR spectroscopic methods have been highly effective in the study of zeolites, but the sizable second-order quadrupolar interaction at Al, which contains higher-rank anisotropic terms, cannot be completely averaged out by MAS. New methods such as double rotation (DOR),[32] dynamic angle spinning (DAS),[33] multiple-quantum (MQ) MAS,[34] and satellite transition (ST) MAS[35] have been proposed to overcome this drawback. Among these, MQ MAS, which was proposed recently by Frydman and Harwood,[34, 36] appears the most promising.[37–40] In this experiment, the second-order quadrupolar broadening effect of half-integer quadrupolar nuclei is refocused by a multiple-quantum transition. When incorporated with MAS NMR experiments, this elegant method disperses chemical shifts in the second dimension[37–41] and thereby demonstrates its potential as a tool for elucidation of chemical structures which result from complex reactions.

In this study ^{27}Al MQ MAS NMR spectroscopy is used to investigate the acid properties and the integrity of chemical species by a comparative study of NH_3 and $(CH_3)_3P$ adsorption experiments on a series of dealuminated MCM-22 zeolites. Significant structural information was obtained by the comparison of their corresponding ^1H MAS, ^{31}P MAS, ^{27}Al MAS, and CP/MAS NMR spectroscopic results from these adsorption studies.

Results

Water-reconstructed surface: The ^{27}Al MAS (9.4 and 19.6 T) and the ^{27}Al CP/MAS (9.4 T) NMR spectra of the parent zeolite **p**, and **h1**, and **h2** (hydrothermally treated MCM-22 samples) are shown in Figure 1. In general, two groups of peaks centered at $\delta = 0$ and ≈ 55 are observed in these spectra (Figure 1a). The former signal is assigned to octahedral Al and the latter to tetrahedral Al. Although these peaks are better resolved at 19.6 T (Figure 1b), in particular the overlapping peaks at $\delta \approx 55$,[9, 11, 42] their spectral quality is not sufficient for complete elucidation of the structure of the various Al species.

The ^{27}Al MQ MAS spectra of **p**, **h1**, and **h2** are presented in Figure 2a–c, respectively. For **p** (Figure 2a), three contour plots which correspond to peaks in the tetrahedral Al^F region (signals A, B, and C) are resolved and one well-defined octahedral Al species (signal D) appears at $\delta = 0$ in the F_2 dimension. The isotropic shift and the second-order quadrupolar effect (SOQE) are estimated from the spectrum with the following Equations (1) and (2) in which $\delta_{iso}(i)$ is the

$$\delta_{iso}(i) = 4/3\delta_1(i) - 1/3\delta_2(i) \quad (1)$$

$$\mathrm{SOQE}(i)^2 = C_q(i)^2(1 + \eta(i)^2)/3 = [\delta_{iso}(i) - \delta_2(i)]\nu_0^2/6000 \quad (2)$$

isotropic chemical shift and $\delta_1(i)$ and $\delta_2(i)$ are the coordinates for the center of gravity of signal i in the F_1 and F_2 dimensions, respectively; $C_q(i)$ is the quadrupolar coupling constant; $\eta(i)$ is the asymmetry parameter; and ν_0 is the Larmor frequency of ^{27}Al..

The NMR properties and their assignment to the corresponding Al species are summarized in Table 1. Although their SOQE values are similar (averaging 1.7 MHz), the dispersion in the chemical shift is sufficiently large to allow resolution of A, B, and C, and their assignment to the isotropic chemical shift of $\delta = 49.6$, 56.9, and 61.3, respectively. The

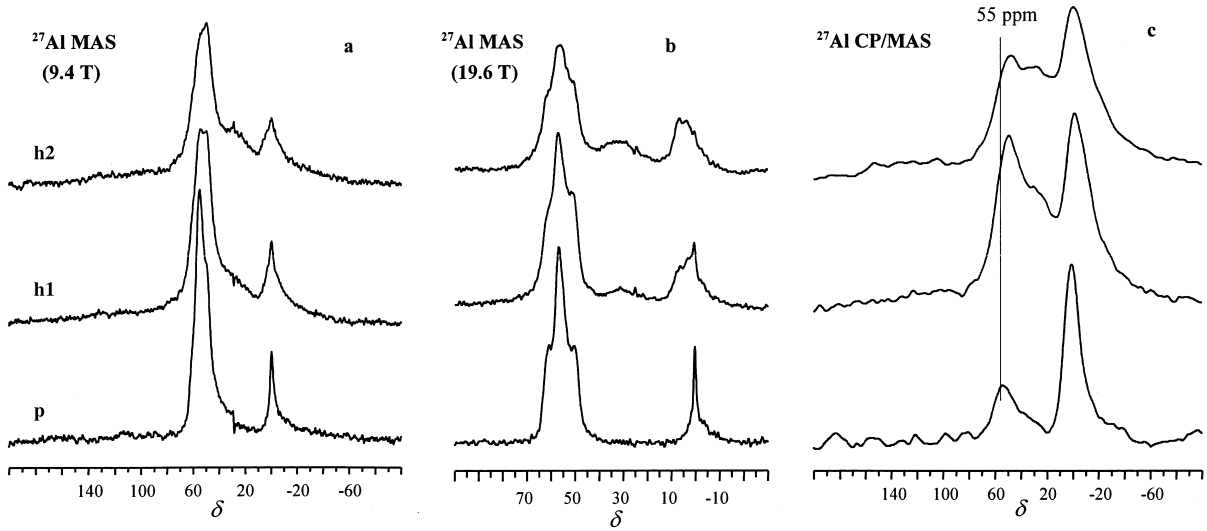

Figure 1. ^{27}Al MAS (9.4 T (a) and 19.6 T (b)) and CP/MAS (c) spectra of parent MCM-22 (**p**), and **p** after hydrothermal treatment at 723 K (**h1**) and 823 K (**h2**). A sharp and a broad signal overlap at $\delta = 0$ in the ultrahigh field ^{27}Al MAS NMR spectra of **h1**. The line-broadening for MAS is 80 Hz, for CP/MAS 300 Hz.

  0947-6539/02/0801-0163 $ 17.50+.50/0

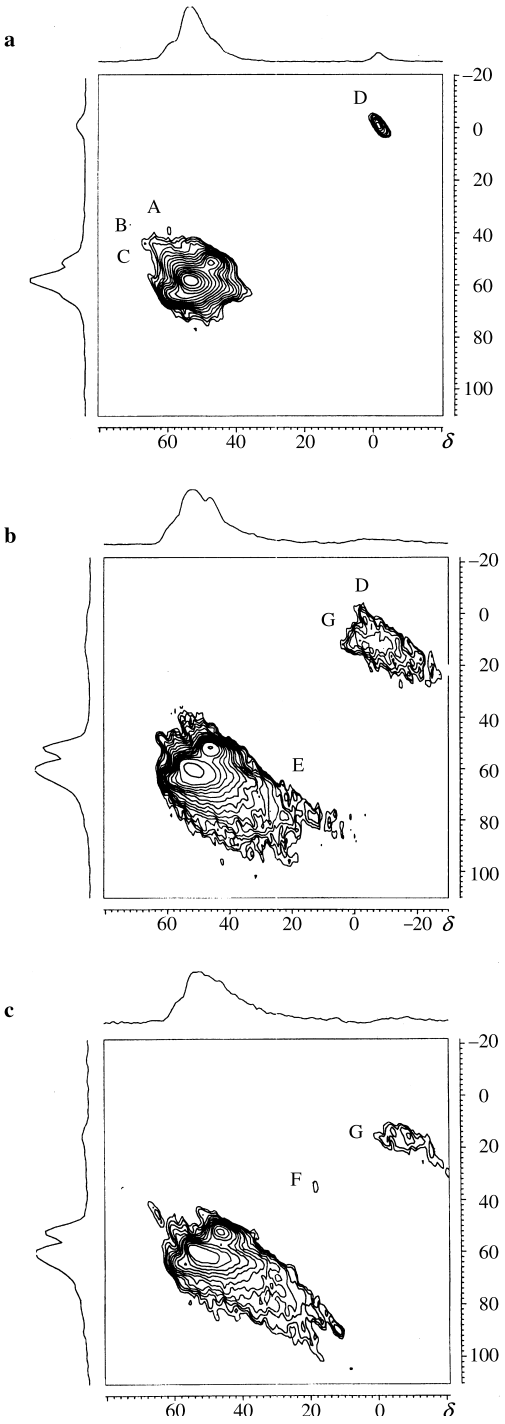

Figure 2. Two-dimesional ^{27}Al MQ MAS NMR spectra of a) **p**, b) **h1**, and c) **h2**.

properties of A, B, and C have been discussed independently by us[16] and by others.[9, 11, 42] These arguments will not be repeated here as their nature remains elusive.

As shown in the isotropic projection of the MQ MAS spectrum in the F_1 dimension (Figures 2b and c), there is a variation in the relative ratio of A, B, and C on hydrothermal treatments. A new signal E (δ_{iso} ^{27}Al = 59.1, SOQE = 5.2 MHz) appears as a tail to A, B, and C and its peak position falls within the Al chemical shift region for tetrahedral Al^F. It is likely that E is a four-coordinate (tetrahedral) Al center

Table 1. The parameters and assignment of different aluminum species.

Signal	Coordination	δ_{iso}	SOQE [MHz]	framework
A	4	49.6	1.52	yes
B	4	56.9	1.71	yes
C	4	61.3	1.89	yes
D	6[a]	−1.9	0.60	yes
E	4	59.1	5.20	yes
F	5	26.7	3.6	no
G	6	5.0	3.7	no
three-coordinate	3	very broad peak	$C_q > 15$ MHz[b]	yes

[a] An aluminum site connected with three water and three (OSi). [b] Reported in refs. [2, 46].

connected to the zeolite framework that is formed during calcination or hydrothermal treatment. Moreover, its SOQE indicates that 1) the electronic environment about the Al is highly distorted and 2) a complex morphology is expected, because there is a distribution of quadrupolar interaction as shown by the lack of significant line narrowing. Fyfe et al.,[43] Grobet et al.[44] and van Boknoven et al.[40] recently reported similar Al species.

Projection to the F_2 dimension gives rise to peaks that span a chemical shift range of $\delta = 20-40$ and superimposes on the chemical shift range of five-coordinate Al^{NF}. At 723 K (**h1**), MQ MAS experiments did not detect five-coordinate Al^{NF}, but a trace amount (signal F in Figure 2c) appeared at higher treatment temperatures. In the study of the zeolite USY by Fyfe et al.,[43] the five-coordinate Al^{NF} is barely visible in the MQ MAS spectrum despite accounting for ≈20% of the total Al content. This result agrees with the NMR data obtained in this study.

From these results, it is suggested that the peak at $\delta \approx 30$ in the one-dimesional spectra is in fact a superposition of peaks which originate from both distorted tetrahedral Al^F (signal E in Figure 2b) and five-coordinate Al^{NF} (signal F in Figure 2c).[1, 16] Under more rigorous hydrothermal treatment, the distorted tetrahedral Al^F gradually transforms to the five-coordinate Al^{NF} as indicated by Figure 2b and c. The signal D → G from octahedral Al broadened significantly (Figure 2a → b) during the hydrothermal treatment of **p**; this suggests the presence of more than one octahedral Al species (vide infra).

In comparison to the ^{27}Al MAS spectra, the ^{27}Al CP/MAS spectrum of **p** (Figure 1c) demonstrated a preferential increase in the intensity of the octahedral Al peak at $\delta = 0$. Since cross-polarization is derived from closely attached hydroxyl groups and/or water molecules, this implies that water is directly bound to Al sites in this fully hydrated sample. The five-coordinate Al^{NF} (δ_{iso} ^{27}Al ≈ 30) that is observed in the corresponding MAS spectra and the two-dimensional MQ MAS spectrum (signal F in Figure 2c) is also resolved in the CP/MAS spectra, therefore, it should also be associated with hydroxyl- or water-bound species.

After the hydrothermal treatment, both the four-coordinate Al^F and octahedral Al peaks had broadened. Furthermore, the intensity of the four-coordinate Al^F peak ($\delta \approx 55$) had increased and its peak shifted to $\delta \approx 47$ in the ^{27}Al CP/MAS spectra (Figure 1c). This result suggests the plausible

0947-6539/02/0801-0164 $ 17.50+.50/0 *Chem. Eur. J.* **2002**, *8*, No. 1

formation of one new Al species, which is hydroxy- or water-bound but ^{27}Al 3Q MAS invisible. Klinowski et al.[1]have demonstrated by quadrupole nutation experiments that both Al^{F} and Al^{NF} could serve as sources for the formation of new tetrahedral Al species. Therefore, both tetrahedral Al^{F} and Al^{NF} species may contribute to the peak observed at $\delta \approx 50$ found in **h1** and **h2**.

We have also demonstrated previously[16] that a broad "hump" between $\delta \approx 100-150$ in the ^{27}Al MAS spectra of fully hydrated and dealuminated samples is assigned to three-coordinate Al^{F} with a large quadrupole coupling constant ($C_q > 15$ MHz). A second broad hump, which is located at a position similar to that described above in the ^{27}Al MAS spectra, is believed to result from the site symmetry lowering of a previously visible aluminum species (either Al^{F} and Al^{NF}) during dehydration, but is eliminated by full rehydration.[16] It is suggested that three-coordinate Al^{F} sites with large C_q are responsible for Lewis acidity in zeolites.[2, 46] However, MQ MAS experiments did not detect three-coordinate Al species; the large quadrupolar interaction ($C_q > 15$ MHz)[2] and very weak intensity would tend to wash out the spectrum and render its MQ MAS invisible. Therefore, MAS, CP/MAS and MQ MAS techniques observes at least five kinds of Al species, namely tetrahedral Al^{F}, distorted tetrahedral Al^{NF}, three-coordinate Al^{F}, five-coordinate Al^{NF}, octahedral Al, and possibly tetrahedral Al^{NF}, in water-reconstructed samples.

^{1}H and ^{31}P MAS NMR spectra of dehydrated samples after TMP or NH_3 adsorption: The ^{1}H MAS NMR spectra of the three samples with and without NH_3 are presented in Figure 3. In the absence of an NH_3 load, four ^{1}H NMR peaks in Figure 3a are assigned to external silanol ($\delta_{iso}{}^{1}H = 1.6$), Al–OH ($\delta = 2.2$), and two kinds of Brønsted hydroxyls[47] ($\delta = 3.8$, 6.0). On completion of hydrothermal treatment, the intensity change of the ^{1}H NMR peaks revealed that a significant gain in the amount of external silanol had occurred with a decrease in the proportion of the two Brønsted acid sites. This result is corroborated by the diminishing intensity of the peak at $\delta_{iso}{}^{31}P = \approx -6$, which is assigned to the formation of $TMPH^{+}$–zeolite complexes upon adsorption of TMP on Brønsted acid sites, in the ^{31}P MAS NMR spectra of **p**, **h1**, and **h2** (Figure 4). Inspection of this ^{31}P peak reveals the presence of two superimposed components similar to those observed by others.[25] This indicates that TMP resides in two types of channels, that is, in two kinds of Brønsted acid sites in MCM-22.[11] No oxides of TMP are detected ($\delta > 10$). This confirms the efficiency of the in-situ apparatus built in this laboratory. After chemisorption of NH_3, species occurring between $\delta_{iso}{}^{1}H = 2-6$ shifted to lower field (Figure 3). With the exception of the external silanol peak at $\delta \approx 1.6$, four peaks at $\delta_{iso}{}^{1}H = 2.8$, 4.6, 5.9, and 6.8 were observed for **p**. The resonance at $\delta = 6.8$ is assigned to NH_3[48], which is adsorbed onto Brønsted sites, that is, an $NH_4{}^{+}$–zeolite complex, and the peak at $\delta = 5.9$ is assigned to $NH_4{}^{+}$, which is involved in fast exchange with $NH_4{}^{+}$ ($\delta = 6.8$), H^{+} ($\delta = 3.7$) and NH_3 ($\delta = 0.8$).[49] The remaining peaks at $\delta = 4.6$ and 2.8 could result from the contribution of NH_3 adsorption onto Lewis acid sites, or to an exchange process between different kinds of species due to the complex nature of NH_3 species adsorbed on the zeolite surface.[50] The signal intensity of the peak at $\delta = 4.6$ passes through a maximum between 723 K (**h1**) and 823 K (**h2**); this corrolates with the behavior of Lewis sites studied by ^{31}P MAS NMR experiments (Figure 4). In Figure 4 (see **h1**), the peak at $\delta_{iso}{}^{31}P = -44$ falls within the chemical shift range of TMP that is adsorbed on Lewis acid sites.[23] The ^{31}P MAS NMR spectra also revealed the presence of a

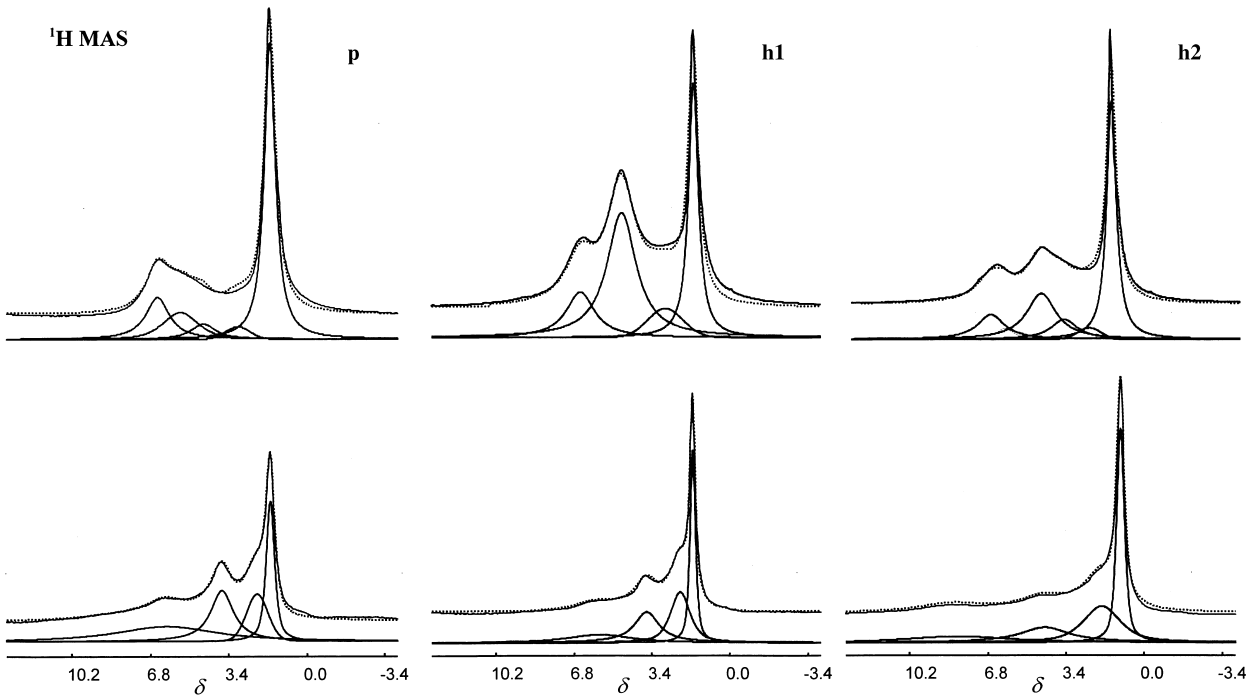

Figure 3. ^{1}H MAS NMR spectra of **p**, **h1**, and **h2** with and without ammonia adsorption. The bottom traces correspond to the spectra of samples before ammonia adsorption, the top traces after ammonia adsorption.

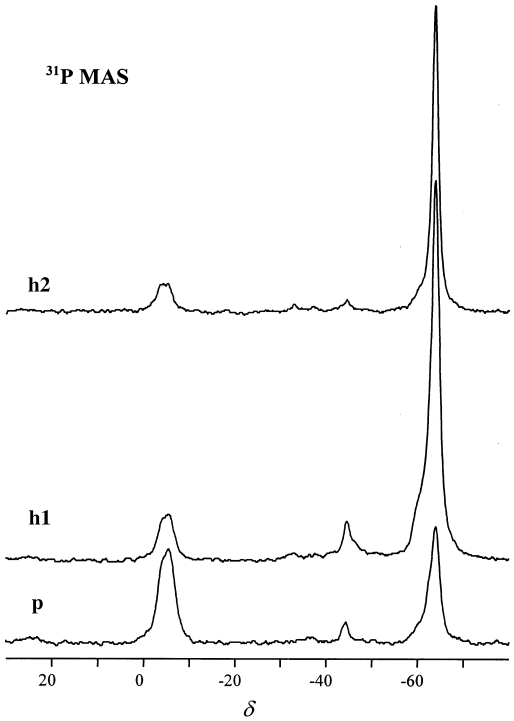

Figure 4. ^{31}P MAS NMR spectra of **p**, **h1**, and **h2** after loading with trimethylphosphine. The resonance assigned to Brønsted acid sites consists of two overlapped signals. No low-field resonance was observed, that is, the peak attributed to adsorbed trimethylphoshpine oxide was not detected and the system was free from oxygen leakage.

shoulder at $\delta_{iso}{}^{31}P = -59$, which appears at lower field to the main peak at $\delta_{iso}{}^{31}P = -65$ in **h1**. While the former is also attributed to TMP that is adsorbed on Lewis acid sites, the latter has been established to arise from a physisorbed TMP peak.[23] Therefore, the two species at Lewis sites which give rise to signals at $\delta_{iso}{}^{31}P = -44$ and -59 behave similarly during hydrothermal treatments, that is, with a decrease in their peak intensity upon reaching 823 K (**h2**) relative to that observed at 723 K (**h1**). These results support the assignment of the peak at $\delta_{iso}{}^{1}H = 4.6$ in the ^{1}H spectra to that of adduct formed from the adsorption of NH_3 on a Lewis acid site. We concluded therefore that there are two types of Brønsted sites and at least two types of Lewis acid sites present in the zeolite MCM-22. The number of Brønsted sites decreased under exposure to high-temperature steam and the maximum number of Lewis sites was reached at a steam temperature of 723 K in the hydrothermal treatment process.

^{27}Al MAS and CP/MAS NMR spectra with NH_3 or TMP loads: Fripiat et al.[20] pointed out that water chemisorption on a zeolite surface involves an unknown number of reconstructed layers due to the dissociative chemisorption behavior of water. As such, water-reconstructed ^{27}Al MAS and CP/MAS NMR results may potentially provide a bias representation of the surface information of zeolite. No signals could be detected in the ^{27}Al NMR spectra when the sample was fully dehydrated at conditions identical to those employed in recording the proton NMR spectra. This suggests that dehydration lowered the symmetry of the Al sites; therefore the three signals at $\delta =$ 0, 30 and 55 are broadened beyond detection. Menorval et al.[51] reported similar results in their study of the dehydration of β-zeolite, and attributed the failure in detecting a NMR signal to peak broadening due to site symmetry lowering at Al of the zeolite lattice upon removal of water molecules. This effect increases the electric-field gradient at Al and causes an increase in the size of the C_q. When NH_3 is adsorbed on the fully dehydrated sample surface, cross-polarization is derived from the chemisorbed NH_3, through which the distribution of surface Al is observed. Ammonia adsorption most likely reduces the electric field gradient at Al and enables surface Al to be detected by MAS experiments.

When dehydrated **p** was loaded with NH_3, a dramatic change occured as compared with its water-reconstructed ^{27}Al MAS NMR spectra. The tetrahedral Al^F peak at $\delta \approx 55$ (signals A, B, and C in Figure 2a) was observed but the octahedral Al species at $\delta = 0$ had disappeared (Figure 5). This result suggests that a transformation to another Al species, probably four-coordinate, has occurred, since the peak at $\delta \approx 55$ is the only signal observed in the ^{27}Al MAS spectrum despite a ± 400 ppm chemical shift scan. This hypothesis is confirmed by examination of the results in the corresponding ^{27}Al CP/MAS NMR spectra (Figure 5). The dominant octahedral Al peak at $\delta = 0$ for the ^{27}Al CP/MAS NMR of water-reconstructed samples (Figure 1) vanished upon loading dehydrated **p** with NH_3. The ^{27}Al MAS NMR spectra of hydrothermally treated samples **h1** and **h2** revealed the presence of a shoulder at $\delta_{iso}{}^{27}Al \approx$ 30, adjacent to the four-coordinate Al^F peak at $\delta \approx 55$, and a broad peak at $\delta_{iso}{}^{27}Al = 0$. Confirmation of their existence could be found in the corresponding ^{27}Al CP/MAS NMR spectra. Moreover, the large hump observed in the ^{27}Al MAS NMR of the fully hydrated **h1** or **h2** samples was not detected in the NH_3-loaded spectra.

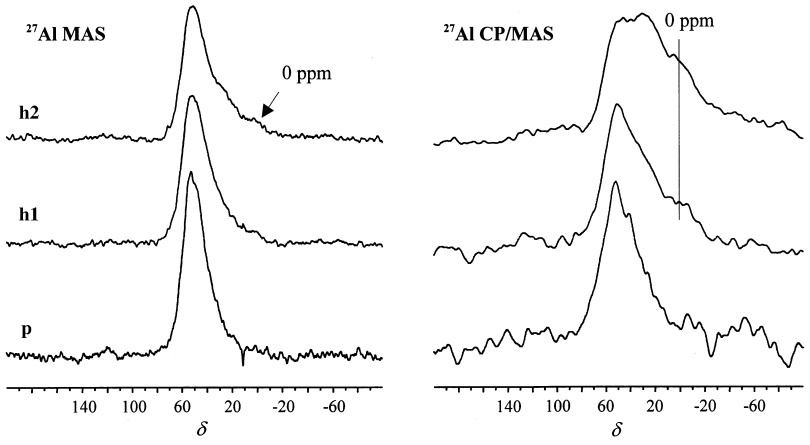

Figure 5. ^{27}Al MAS (9.4 T) and CP/MAS spectra of dehydrated **p**, **h1**, and **h2** after loading with ammonia. For **h1**, the narrow line at $\delta = 0$ is absent, while the broad peak remains unchanged.

0947-6539/02/0801-0166 $ 17.50+.50/0 *Chem. Eur. J.* **2002**, *8*, No. 1

The ^{27}Al MAS and CP/MAS NMR spectra (Figure 6) of TMP-loaded samples exhibit features similar to those observed for NH_3-loaded samples. This can be easily rationalized as both molecules are basic and, hence, their interactions with acid sites would occur in a similar manner. The intensities of the ^{27}Al MAS NMR spectra of **h1** and **h2** decrease substantially relative to those of the water-reconstructed surface. For **h1**, about 40 % of the Al is NMR invisible due to its low symmetry in the fully dehydrated form and to its nonassociation with TMP molecules. Distortion of zeolite channels together with the dislodgment of Al from the lattice may block or hinder the contact of large probe molecules such as TMP with Al within zeolite channels. As a consequence, the number of acid sites in zeolites is underestimated. This is in agreement with the quantitative TMP adsorption study carried out by Lunsford et al.[28]

Discussion

When a basic ligand, L (including water), is adsorbed on the zeolite surface, it reacts with both the Brønsted, to form Si–OHL–Al, and Lewis acid sites. A comparison between the ^{27}Al MAS and CP/MAS NMR spectra of hydrated and ammonia-adsorbed zeolite samples (Figures 1 and 5) reveals that: 1) Al is invisible to ^{27}Al MAS NMR in the case of strictly dehydrated zeolite samples and 2) once the adsorbent is loaded, the electric-field gradient at Al is sufficiently reduced to render Al to be detectable by NMR spectroscopy. In water-loaded ^{27}Al MAS and MQ MAS spectra of **p**, there are both tetrahedral Al^F and octahedral Al species. We conclude from the corresponding ^{27}Al CP/MAS NMR spectral information that the octahedral species is highly associated with water. From the ammonia-adsorbed ^{27}Al MAS and CP/MAS NMR spectral information of **p**, a unique peak at $\delta = 55$ from tetrahedral Al is observed that suggests that transformation of octahedral Al to tetrahedral Al has occurred.

Bourgeat-Lami et al.[52] first reported that for β-zeolite, the thermal decomposition of its ammonium form yields a material that contains distorted tetrahedral Al atoms, which subsequently transform to octahedral Al atoms in the presence of water. This process is reversible and the tetrahedral Al atom is recovered in its distorted form once NH_3 is absorbed. The authors attributed this unique property to the special crystallographic structure present in the β-zeolite framework. Subsequent studies on Y[53] and ZK-4[54] suggest that this unusual property is probably a general characteristic possessed by most zeolites. From an analysis of quantitative temperature-programmed ammonia desorption (TPAD), ^{27}Al MAS, ^{29}Si MAS NMR, and IR spectra, Woolery et al.[55] concluded that partial hydrolysis of framework Al–O bonds, which leads to the formation of $Al(OSi)_3$ moiety, is responsible for the transformation of framework Al between the tetrahedral and octahedral forms. Absorbtion of NH_3 gives $Al(OSi)_3$–NH_3, whereas $Al(OSi)_3(H_2O)_3$ is formed when the zeolite is fully hydrated. From our results, we conclude octahedral Al in the parent zeolite MCM-22 does not originate from nonframework species. Instead, Al is connected to the zeolite lattice and recovers its tetrahedral form when NH_3 is chemisorbed. The three-coordinate Al species are responsible for the Lewis sites observed during base adsorption. When the ammonia-loaded sample is fully rehydrated in a water-saturated deccicator, the peak at $\delta = 0$ reappears; this implies that coordination with water results uniquely in octahedral Al. When methanol was used as adsorbent, Menorval et al.[51] reported that octahedral Al^F in β-zeolite was observed after the sealed rotor was heated at 470 K for 30 min. Under these conditions, water is generated in-situ from the condensation reaction of methanol. The reappearance of the octahedral Al species is therefore attributed to water adsorption on specific tetrahedral Al sites as ligands in the first coordination sphere, since it is well known that Lewis acid type Al has a greater affinity for oxygen-containing ligands as adsorbents.

For **h1** and **h2**, the NH_3-adsorbed ^{27}Al MAS NMR spectra (Figure 5) are completely different in comparison to those of the water-loaded samples (Figure 1). The presence of five-coordinate Al^{NF} (or distorted tetrahedral Al^{NF}) and octahedral Al, while detected in small amounts by ^{27}Al MAS NMR, is more apparent in their corresponding ^{27}Al CP/MAS spectra. However, the low intensity of octahedral Al in the ^{27}Al CP/MAS spectrum of dealuminated, ammonia-loaded samples, as compared with that of water-loaded samples, indicates that the coordination number or the amount of ammonia as nearest neighbor on these Al sites may be lower than that found for zeolites loaded with water. Moreover, the broad hump observed in the water-reconstructed ^{27}Al MAS NMR spectra of **h1** or **h2** disappeared after ammonia was loaded. These observations can be understood with the following explanation: after hydrothermal treatment, water-loaded zeolites contain a proportion of octahedral Al species that function as Lewis

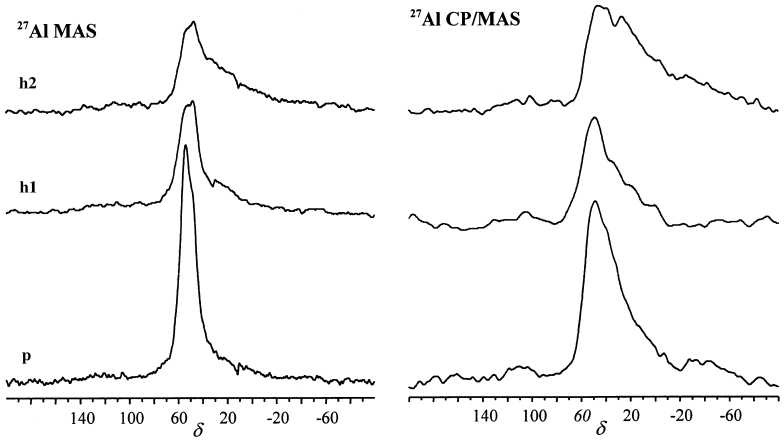

Figure 6. ^{27}Al MAS (9.4 T) and CP/MAS spectra of dehydrated **p**, **h1**, and **h2** after loading with trimethylphosphine.

acid sites and that transform into tetrahedral Al once ammonia is loaded (see Figures 1 and 5). This species remains in the framework as a result of the partial hydrolysis of Al–O bonds during hydrothermal treatment. As shown in Figures 1 and 5, most of the octahedral Al in **p** is in this state. The octahedral Al, which remains unchanged (see **h1** and **h2** spectra in Figure 5), is nonframework and cannot be restored to its tetrahedral geometry with ammonia adsorption. Although these two kinds of octahedral aluminums cannot be distinguished at 9.4 T, they are resolved at ultrahigh field (19.6 T) by ^{27}Al MAS (Figure 1b) and ^{27}Al ST MAS NMR spectra (see Supporting Information).

A very sharp peak at $\delta_{iso}{}^{27}\mathrm{Al} = 0$ in Figure 1b for **p** corresponds to an octahedral Al^F species, and two overlapped signals (one narrow and one broad) are discernible in the spectrum of **h1**. The broad peak, which is assigned to the nonframework octahedral Al species, does not change on ammonia adsorption (Figure 5). Two-dimensional MQ MAS provides another verification of the presence of two different octahedral Al species. For the parent zeolite, the uniform octahedral Al species is observed at $\delta_{iso}{}^{27}\mathrm{Al} = -1.9$ with a SOQE of 0.6 MHz, whereas the second octahedral Al^{NF} species ($\delta_{iso}{}^{27}\mathrm{Al} = 5.0$) is expected to have a highly distorted electronic environment based on its large quadrupole coupling (SOQE $\approx$ 3.7 MHz). Also, the Al probably cannot coordinate directly to ammonia; this results in a relatively lower intensity in the ^{27}Al CP/MAS spectrum relative to those of water-loaded samples.

A recent study by Kuehl and Timken[56] on the β-zeolite also reports the detection of distinct octahedral Al^F species and a nonframework species. They found that the higher the hydrothermal treatment temperature, the smaller the amount of octahedral Al^F, and the higher the amount of octahedral Al^{NF} formed. This implies that the octahedral Al^F will eventually become nonframework species because of the continuing hydrolysis of the remaining framework Al–O bonds under more rigorous conditions. The disappearance of the broad hump in the ^{27}Al spectrum indicates that three-coordinate Al is converted to tetrahedral Al upon coordination with an ammonia molecule. This three-coordinate Al species is expected to have a highly distorted geometry as illustrated by its large C_q ($>$15 MHz). It has been suggested that three-coordinate Al is the Lewis acid site in thermal or hydrothermally treated zeolites[46] and our results support this conclusion.

The maximum number of the TMP–L or the NH_3–L adducts in **h1**, which is observed in both the ^{31}P MAS and ^{1}H MAS NMR spectra, confirms the origin of Lewis acid sites. Both octahedral Al^F and three-coordinate Al^F species contribute to the Lewis acidity. The parent MCM-22 (**p**) contains mainly octahedral Al^F, whereas the zeolite treated with high-temperature steam (**h2**) contains mainly three-coordinate Al. Both Al species are responsible for the Lewis acidity of a zeolite treated with steam at a moderate temperature (**h1**). These results thus account for the existence of an observed maximum in the NMR peak intensity (Figures 3 and 4) on going from the parent zeolite (**p**) to 723 K (**h1**) to 823 K (**h2**).

Finally, the theory that the ^{27}Al resonance at $\delta \approx 30$ (an overlap of distorted tetrahedral Al^F species and five-coordinate Al^{NF}) in a hydrothermally treated sample may also contribute to Lewis acid sites cannot be confirmed in this study. Further investigation with the recently introduced technique, that is, ^{15}N–^{27}Al MQ HETCOR experiments,[57] may clarify the controversy as to whether or not these sites are Lewis centers.[56]

Conclusion

This study shows that the zeolite MCM-22 contains two kinds of Lewis acid sites. Through a comparative study of the water-loaded or ammonia/TMP-adsorbed ^{27}Al MAS and CP/MAS NMR spectra, these sites are confirmed to be an octahedral Al^F (which is three-coordinate in nature) and three-coordinate Al. The former is generated during calcination and results from partial hydrolysis of framework Al–O bonds, which transform into tetrahedral Al^F upon NH_3 or TMP adsorption. This octahedral Al^F species is further hydrolyzed by increasing the hydrothermal treatment temperature and converts to octahedral Al^{NF}. It cannot be restored to its initial tetrahedral geometry by ammonia adsorption. The highest density of Lewis acid sites is observed on samples treated at a moderate temperature, since both Al species contribute to the Lewis acidity. The question as to whether the distorted tetrahedral Al^F resolved by ^{27}Al MQ MAS NMR methods contributes to Lewis acidity requires additional investigation.

As indicated by the ^{27}Al MAS NMR results, TMP does not come into contact with all Al atoms in the zeolite lattice, especially in dealuminated samples, due to the steric restrictions of the large TMP molecule. While steric hindrance does not affect ammonia adsorption on zeolite, it remains difficult to obtain conclusive information on Brønsted or Lewis acidity from either ^{1}H or ^{15}N NMR methods. This is due to the relatively small ^{1}H chemical shift range and the low natural abundance of the ^{15}N nuclei. As revealed in Figures 1 and 3, Lewis acid sites in zeolite can be readily created by controlling thermal or hydrothermal treatment conditions. Further investigation is required in order to determine precisely the different roles Lewis acid sites may play in a specific reaction.

Experimental Section

Materials: MCM-22 zeolite (Si/Al = 15) was synthesized with hexamethyleneimine (HMI) as the directing agent.[14] The crystalline structure (MWW) of the synthesized zeolite was measured by XRD (D/max–rB diffractometer, $Cu_{K\alpha}$ radiation). No hybrid crystallites were observed. The proton form of the zeolite (denoted as **p**) was obtained by three-fold successive exchange with 1M NH_4NO_3 solution at 363 K. The product was washed and dried at 373 K, heated to 823 K at 10 K min^{-1}, and kept at 823 K for 4 h. The hydrothermally treated samples, that is, **h1** and **h2**, were obtained by treating the samples under water vapor (4 mL h^{-1} $g_{zeolite}^{-1}$) at 723 and 823 K, respectively, for 2 h.

Adsorption: A custom-designed apparatus used to conduct dehydration and/or adsorption experiments of zeolite was described previously.[17] After dehydration/adsorption, the sample was transferred in-situ into an NMR rotor, and sealed under in the absence of air and moisture. ^{1}H NMR experiments have demonstrated that the packing procedure of the rotor was effective, since leakage of moisture from the atmosphere was not detected within 48 h. Before adsorption, the zeolite samples were evacuated under 10^{-2} Pa at 723 K for 20 h, and the resulting materials

  0947-6539/02/0801-0168 $ 17.50+.50/0 *Chem. Eur. J.* **2002**, *8*, No. 1

were characterized by ^{1}H MAS NMR spectroscopy. The samples were placed in a Schlenk line and exposed to 40 Torr of TMP (trimethylphosphine, Acros) at room temperature for 30 min. Excess TMP was removed by evacuating the samples at 323 K for 10–20 min and sealed for NMR measurement. The dehydration process is identical for NH_3 adsorption experiments to that described above, except that anhydrous ammonia (50 Torr) was introduced into the system at 388 K and held for 30 min. Physisorbed NH_3 was removed by outgassing at the same temperature for half an hour.

NMR measurements: ^{27}Al NMR spectra were recorded on Bruker spectrometers at 7.05 T at 78.2 MHz (ASX-300), 9.4 T at 104.3 MHz (DRX-400), and 19.6 T operating at 217.62 MHz (DRX-833). For ^{27}Al 3Q MAS NMR spectra recorded at 7.05 T, the 4 mm rotors were spun at 12 kHz. To produce pure-absorption line shapes, a simple two-pulse sequence was used and the conditions for excitation and transfer of the ($\pm$3Q) coherence were optimized. The phase cycle was composed of six phases for the selection of the triple-quantum coherence, and was combined with a classic overall four-phase cycle to minimize phase and amplitude missetting of the receiver. A recycling time of 0.5 s was used, as the relaxation of ^{27}Al in solid is generally fast. A 12 μs increment was used for 3Q MAS. The $t_2 \times t_1$ matrix was 512×256 and F_1 dimensions were zero-filled to 512 points. All pulse durations were optimized by taking the excitation and detection pulse at 3 μs and 1 μs. The radio frequency field strength was 143 kHz. 420 transients were taken for the experiments. After 3Q MAS measurements were completed, "shearing" was performed by using an in-house program.[41] The chemical shift was referenced to $[Al(H_2O)_6]^{3+}$. For ^{27}Al MAS NMR spectra, which were recorded at 9.4 T using a single pulse, the pulse width was set at 0.75 μs (π/12) and 800 scans were accumulated. A 3 s relaxation delay was determined to be sufficiently long to permit quantitative analysis of zeolite sample. 1% aqueous $[Al(H_2O)_6]^{3+}$ was used as the chemical shift reference and samples were spun at 8 kHz by using 4 mm ZrO_2 rotors. For ^{27}Al MAS recorded at 19.6 T, the measurements were performed with a spin rate of 19.1 kHz, 2 μs excitation pulse, 5 s recycle delay, and 512 scans.

^{1}H MAS NMR spectra were collected at 400.1 MHz using single-pulses with the π/10 pulse set at 1 μs and a 4 s recycle delay was used. The ^{1}H spectra were accumulated for 200 scans and the rotor was spun at 8 kHz. The chemical shifts were referenced to a saturated aqueous solution of sodium 4,4-dimethyl-4-silapentane sulfonate (DSS). For $^1H \rightarrow {}^{27}Al$ CP/MAS NMR measurements, the spectra were recorded with a single contact with an optimized contact time of 1.2 ms, a cycle delay of 4 s, and MAS at 10 kHz. The Hartmann–Hahn condition was established in one scan on a sample of pure and highly crystalline kaolinite with similar acquisition parameters. Since resonance is only allowed for the central ($-1/2 \leftrightarrow +1/2$) transition, excitation is selective, and, therefore, the Hartmann–Hahn condition is $3\gamma_{Al}B_{Al} = \gamma_H B_H$, in which γ_{Al} and γ_H denote the gyromagnetic ratios of ^{27}Al and ^{1}H, respectively, and B is the radiofrequency field strength. To obtain a satisfactory signal–noise ratio, 15000–16000 scans were accumulated.

^{31}P MAS NMR spectra were also recorded at 9.4 T and 161.9 MHz. The spectra were obtained using a 2 μs (π/6) pulse and 2 s recycle delay. 1000 scans were accumulated at a the spinning rate of 5 kHz. Chemical shifts were referenced to 85% H_3PO_4.

Acknowledgement

Financial support from the National Natural Science Foundation of China and the Ministry of Science and Technology of China, Project No. G1999022400, is gratefully acknowledged.

[1] J. Rocha, S. E. Carr, J. Klinowski, *Chem. Phys. Lett.* **1991**, *187*, 401.
[2] F. Deng, Y. Du, C. Ye, J. Wang, T. Ding, H. Li, *J. Phys. Chem.* **1995**, *99*, 15208.
[3] L. Kellberg, M. Linsten, H. J. Jakobsen, *Chem. Phys. Lett.* **1991**, *182*, 120.
[4] L. Beck, J. F. Haw, *J. Phys. Chem.* **1996**, *100*, 465.
[5] W. O. Hagg, R. M. Lago, P. B. Weisz, *Nature* **1984**, *309*, 1984; J. Klinowski, J. M. Thomas, C. A. Fyfe, G. C. Gobbi, *Nature* **1982**, *296*, 533.
[6] H. C. Karge, *Catalysis and Adsorption by Zeolites* (Eds.: G. Ohlmann, H. Pfeifer, R. Fricke), Elsevier, Amsterdam, **1991**, p. 133.
[7] M. Rubin, P. Chu, US Patent 4954325, **1990**.
[8] M. E. Leonowicz, J. A. Lawton, S. L. Lawton, M. K. Rubin, *Science* **1994**, *264*, 1910.
[9] G. J. Kennedy, S. L. Lawton, M. K. Rubin, *J. Am. Chem. Soc.* **1994**, *116*, 11000; S. L. Lawton, A. S. Fung, G. J. Kennedy, L. B. Alemany, C. D. Chang, G. H. Hatzikos, D. N. Lissy, M. K. Rubin, H. C. Timken, S. Steuernagel, D. E. Woessner, *J. Phys. Chem.* **1996**, *100*, 3788.
[10] A. Corma, C. Corell, J. Pérez-Pariente, *Zeolites* **1995**, *15*, 2.
[11] W. Kolodziejski, C. Zicovich, C. Corell, J. Pérez-Pariente, A. Corma, *J. Phys. Chem.* **1995**, *99*, 7002.
[12] A. Corma, C. Corell, F. Flopis, A. Martínez, J. Pérez-Pariente, *Appl. Catal. A* **1994**, *115*, 121.
[13] M. J. Verhoef, E. J. Creyghton, J. A. Peters, H. van Bekkum, *Chem. Commun.* **1997**, 1989.
[14] Y. Shu, D. Ma, L. Xu, Y. Xu, X. Bao, *Catal. Lett.*, in press; D. Ma, Y. Shu, M. Cheng, Y. Xu, X. Bao, *J. Catal.* **2000**, *194*, 105.
[15] G. D. Pirngruber, K. Seshan, J. A. Lercher, *J. Catal.* **2000**, *190*, 396.
[16] D. Ma, F. Deng, R. Fu, X. Han, X. Bao, *J. Phys. Chem. B* **2001**, *105*, 1770.
[17] W. Zhang, D. Ma, X. Liu, X. Liu, X. Bao, *Chem. Commun.* **1999**, 1091; D. Ma, Y. Shu, W. Zhang, W. Han, Y. Xu, X. Bao, *Angew. Chem.* **2000**, *112*, 3050; *Angew. Chem. Int. Ed.* **2000**, *39*, 2928.
[18] M. Hunger, D. Freude, H. Pfeifer, *J. Chem. Soc. Faraday Trans.* **1991**, *87*, 657.
[19] P. A. Jacobs, K. Beyer, *J. Phys. Chem.* **1979**, *83*, 1174.
[20] D. Coster, A. L.Blumenfeld, J. J. Fripiat, *J. Phys. Chem.* **1994**, *98*, 6201.
[21] H. D. Morris, P. D. Eilis, *J. Am. Chem. Soc.* **1989**, *111*, 6045.
[22] G. E. Maciel, J. F. Haw, I. S. Chuang, B. L. Hawkins, T. E. Early, D. R. Mckay, L. Petrakis, *J. Am. Chem. Soc.* **1983**, *105*, 5529.
[23] W. P. Rothwell, W. Shen, J. H. Lunsford, *J. Am. Chem. Soc.* **1986**, *106*, 2452; J. H. Lunsford, W. P. Rothwell, W. Shen, *J. Am. Chem. Soc.* **1985**, *107*, 1540.
[24] J. F. Haw, I. S. Chuang, B. L. Hawkins, G. E. Maciel, *J. Am. Chem. Soc.* **1983**, *106*, 7206.
[25] B. Hu, I. D. Gay, *Langmuir* **1999**, *15*, 477.
[26] W. L. Earl, P. O. Fritz, A. A. V. Gibson, J. H. Lunsford, *J. Phys. Chem.* **1987**, *91*, 2091.
[27] J. P. Osegovic, R. S. Drago, *J. Phys. Chem. B* **2000**, *104*, 147.
[28] J. H. Lunsford, P. N. Tutunjian. P. Chu, E. B. Yeh, D. J. Zalewski, *J. Phys. Chem.* **1989**, *93*, 2590.
[29] B. Zhao, H. Pan, J. H. Lunsford, *Langmuir* **1999**, *15*, 2761.
[30] H. Kao, C. Grey, *Chem. Phys. Lett.* **1996**, *259*, 459.
[31] H. Kao, H. Liu, J. Jiang, S. Liu, C. P. Grey, *J. Phys. Chem. B* **2000**, *104*, 4923.
[32] A. Samoson, E. Lippmaa, A. Pines, *Mol. Phys.* **1988**, *65*, 1013.
[33] A. Llor, J. Virlet, *Chem. Phys. Lett.* **1988**, *152*, 248.
[34] L. Frydman, J. S. Harwood, *J. Am. Chem. Soc.* **1995**, *117*, 5367.
[35] Z. Gan, *J. Am. Chem. Soc.* **2000**, *122*, 3242.
[36] A. Medek, J. S. Harwood, L. Frydman, *J. Am. Chem. Soc.* **1995**, *117*, 12779.
[37] C. Fernandez, J. P. Amoureux, *Chem. Phys. Lett.* **1995**, *242*, 449.
[38] J. P. Amoureux, C. Fernandez, S. Steuernagel, *J. Magn. Reson. A* **1996**, *119*, 280.
[39] T.-H. Chen, B. H. Wouters, P. J. Grobet, *J. Phys. Chem. B* **1999**, *103*, 6179.
[40] J. A. Van Bokhoven, A. L. Roest, D. C. Koningsberger, J. T. Miller, Nachtegaal, A. P. M. Kentgens, *J. Phys. Chem. B* **2000**, *104*, 6743.
[41] J. C. C. Chan, *Concepts Magn. Reson.* **1999**, *11*. 363.
[42] M. Hunger, S. Ernst, Weitkamp, *J. Zeolites* **1995**, *15*, 188.
[43] C. A. Fyfe, J. L. Bretherton, L. Y. Lam, *Chem. Commun.* **2000**, 1575.
[44] T.-H. Chen, B. H. Wouters, P. J. Grobet, *Eur. J. Inorg. Chem.* **2000**, 281.
[45] C. P. Grey, A. J. Vega, *J. Am. Chem. Soc.* **1995**, *117*, 8232.
[46] F. Deng, Y. Yue, C. Ye, *Solid State Nucl. Magn. Reson.* **1998**, *10*, 151.
[47] M. Hunger, *Catal. Rev. Sci. Eng.* **1997**, *39*, 345.
[48] F. Yin, A. L. Blumenfeld, V. Gruver, J. J. Fripiat, *J. Phys. Chem. B* **1997**, *101*, 1824.
[49] W. P. J. H. Jacobs, J. W. De Haan, L. J. M. van de Ven, R. A. van Santen, *J. Phys. Chem.* **1993**, *97*, 10394.
[50] D. Michel, A. Germanus, H. Pfifer, *J. Chem. Soc. Faraday Trans.* **1982**, *78*, 113.

[51] L. C. Menorval, W. Buckermann, F. Figueras, F. Fajula, *J. Phys. Chem*. **1996**, *100*, 465.
[52] E. Bourgeat-Lami, P. Massiani, F. D. Renzo, P. Espiau, F. Fajula, *Appl. Catal*. **1991**, *72*, 139.
[53] B. H. Wouters. T. -H. Chen, P. J. Grobet, *J. Am. Chem. Soc*. **1998**, *120*, 11 419.
[54] R. H. Jarman, *Mater. Res. Soc. Symp. Proc*. **1988**, *111*, 119.
[55] G. L. Woolery, G. H. Kuehl, H. C. Timken, A. W. Chester, J. C. Vartuli, *Zeolites* **1997**, *19*, 288.
[56] G. H. Kuehl, H. K. C. Timken, *Microporous Mesoporous Mater*. **2000**, *35*, 521.
[57] S. H. Wangm, S. M. De Paul, L. M. Bull, *J. Magn. Reson*. **1997**, *125*, 364.

Received: June 6, 2001 [F3316]

  0947-6539/02/0801-0170 $ 17.50+.50/0